Low-cost Underwater Localisation Using Single-Beam Echosounders and Inertial Measurement Units

Abu Bakr Azam
MAE, ERI@N (IGS), SNJL
NTU
Singapore
abubakr002@e.ntu.edu.sg

Ze Jie Kong
MAE
NTU
Singapore

Sing Yew Ng
MAE
NTU
Singapore

Michael Scherrer Florian
Mechanical Engineering
OST
Switzerland

Basman Elhadidi
School of Engineering and Digital Science
Nazarbayev University
Kazakhstan

Gerald Seet
MAE, SNJL
NTU
Singapore

Jianmin Zheng
SCSE
NTU
Singapore

Yiyu Cai
MAE, ERI@N, SNJL
NTU
Singapore

***Abstract*—Underwater robot localisation is challenging as it cannot rely on sensors such as the GPS due to electromagnetic wave attenuation or optical cameras due to water turbidity. SONARs are immune to these issues, hence they are used as alternatives for underwater navigation despite lower spatial and temporal resolution. Single-beam SONARs are sensors whose main output is distance. When combined with a filtering algorithm like the Kalman filter, these distance readings can correct localisation data obtained by inertial measurement units. Compared to multi-beam imaging SONARs, the single-beam SONARs are inexpensive to integrate into underwater robots. Therefore, this study aims to develop a low-cost localisation solution utilizing single-beam SONARs and pressure-based depth sensors to correct dead-reckoning linear localisation data using Kalman filters. From experiments, a single-beam SONAR per degree of freedom was able to correct localisation data, without the need of complicated data fusion methods.**

***Index Terms*—Kalman filter, Localisation, SONAR, Underwater robot**

I. Introduction

Underwater robots (UWRs) are used for many inspection and intervention tasks usually carried out by human divers. Examples of these include underwater pipeline inspection, valve turning and aquatic life monitoring. The performance of UWRs to complete such objectives mainly relies on their ability to navigate in given environments. A prerequisite towards great navigational capabilities is to equip UWRs with a robust localisation framework.

Due to the severe attenuation of electromagnetic waves underwater, the use of Global Positioning Satellites (GPS) to navigate is impossible for UWRs. Therefore, inertial measurement units (IMUs) are combined with other sensors, for instance, the Doppler Velocity Log (DVL) to navigate by predicting the future position of the vehicle i.e., dead-reckoning. Additionally, there is a growing interest on perception sensors such as optical cameras to perform visual odometry. Sensor fusion attempts are performed to overcome the errors observed in IMUs due to sensor drift. However, fusing such sensors have some issues, for example, the size and the cost of a DVL or the inability of optical cameras to work in turbid water situations [1].

Acoustic modality is used by aquatic animals as a means of communication and navigation (echolocation), which is immune to the effects of water turbidity and refraction that optical cameras might encounter. Sound Navigation and Ranging (SONAR) sensors work on similar principles utilizing high frequency sounds. SONARs are of various types, like the side-scan variants which are used to observe the seabed and the Forward Looking variants which can create two-dimensional SONAR images. These types of sensors fall under the multi-beam category, which are expensive and heavy for smaller UWRs to use. In contrast, single-beam SONARs are cheaper and lighter than their multi-beam counterparts. The single-beam echosounder from Blue Robotics [2] is an example of such.

Despite its issues, single-beam SONARs can provide distance information for several meters and are immune to water turbidity. As the cost per unit is less, multiple single-beam SONARs can be used in a single UWR to improve its navigational capabilities, mainly to correct the erroneous readings that an IMU would provide.

This study focuses on how distance readings from single-beam SONARs can be combined with readings from the IMU in an attempt to correct the localisation data. The use of single-beam SONARs as viable alternatives for navigation especially when utilizing multiples of such sensors was addressed using relevant literature. This is followed by the experimental setup, complete with the experimental rig specifications and the linear Kalman filter (KF) definitions to ensure repeatability. Finally, the experimental results are presented where its anal-

ysis proves the efficacy of the proposed localisation system.

II. Related Work

A. Single-beam SONARs for navigation

Single-beam SONARs and similar sensors in earlier literature were commonly referred to as pencil-beam SONARs, based on the beam shape. Caccia et al. [3]–[5] used high-frequency single-beam SONARs that could rotate, similar to modern-day mechanical scanning inference SONARs (MSIS). The objective of their works was to navigate UWRs with the help of acoustic devices that could keep track of objects like the seabed or man-made structured environments, e.g., a swimming pool. The linear (for vehicle heading) and extended KFs (for motion estimation with range and bearing information from SONARs) were implemented for navigation.

Fairfield et al. [6], [7] used such SONARs for navigation, especially in more unstructured environments like cave systems. Their UWRs utilized a stack of SONARs arranged in a circular fashion in three major orientations. Several SONARs provide a large field of view (FOV) that helps to keep previously visited features in view. Navigation was done using particle filtering based Simultaneous Localisation and Mapping (SLAM), wherein predictions from devices such as IMUs and DVLs were corrected with SONAR data.

Calado et al. [8] implemented a single-beam SONAR with a range of 50m and FOV of a 10^0, i.e., a low-cost solution to develop a mapping and obstacle avoidance framework. A grid-based map of the obstacles was generated with erroneous SONAR readings and a complex control system was used to avoid them.

Previous work is indicative of similar motivations and methodology when compared with this study. Device and computational inabilities experienced in past works may no longer be applicable now, e.g., Kartal et al. [9] in their work explored the possibility of collecting bathymetric data from seabeds sloped in two axes using one single-beam SONAR. Simulations, powerful computing, and the ease of conducting real-life experiments makes it possible to conduct such studies.

B. Single-beam SONARs as ideal low-cost equipment

The cost of a UWR fleet is influenced by the type of sensors utilized; using all types of sensors will give the best navigational capabilities. However, in an effort to reduce costs, more works tend to utilize inexpensive acoustic devices like single-beam SONARs to achieve long-term navigation.

Tan et al. [10] used single-beam SONARs in multiple UWRs to localise in underwater environments where the bathymetric map was available. Such vehicles communicated via acoustic modems to share localisation information which improved the overall positioning of the fleet. This form of navigation is termed as terrain aided navigation (TAN).

Multiple single-beam SONARs can seemingly perform similar to multi-beam SONARs with regards to navigation. For example, in the case of TAN, Ostermann and Rhen [11] compared the feasibility of using multiple single-beam SONARs instead of FLSs or just one single-beam SONAR. With the help of particle filters, either sensor setup worked well to correct dead-reckoning data but the highlight of their work was that it proved the effectiveness of multiple single-beam SONARs to provide data correction capabilities similar to multi-beam SONARs. Additionally, Morency et al. [12] highlighted the efficacy in utilizing three single-beam SONARs instead of using one for the case of obstacle avoidance. In both cases, the SONARs were separated by some angle and were pointed to a specific direction.

Roznere et al. [13] used the single-beam SONAR to fuse monocular camera images with its distance readings to improve the working of the UWR's SLAM system. It projected the cone of the SONAR beam as a circle on the camera's image to enhance the perception of depth and the scale of the observed object. The inferred depth data was also beneficial in de-noising the optical images obtained in turbid environments. Yang et al. [14] in their article utilized similar single-beam SONARs for obstacle avoidance. A relative depth image was inferred from the optical camera's image with the help of a deep learning model, which was fused with other types of data like the SONAR's distance and the "goal" position for navigation. These were the inputs for a deep reinforcement learning (DRL) model which was task to navigate a UWR around obstacles. Amongst different learned DRL policies, the one that included SONAR's readings performed the best.

III. Methods

A. Experimental setup

Fig. 1 shows the experimental setup for the localisation experiments. An UWR rig is tugged by a stepper motor in a controllable manner. The main devices selected for this study were the WITMotion WT901C IMU [15] and the Blue Robotics single-beam echosounder [2]. A time-of-flight (TOF) sensor (Nooploop TOFSense [16]) was initially used to acquire ground truth data to compare with the filtered data, with the sensor being placed above the water's surface. However, subsequent experiments discarded its use in favour of the stepper motor data. The orientation readings were recorded from the IMU itself and depth readings from a pressure-based depth sensor (Blue Robotics Bar02 [17]).

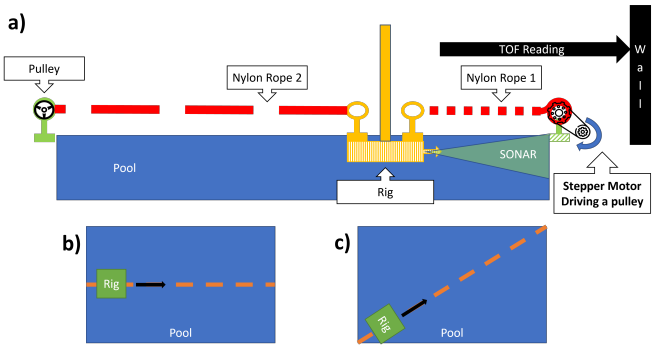

Fig. 1. A simplified experimental setup; a) placement of different experimental equipment; b) 1 DOF experiment plan (surge); c) 2 DOF experiment plan (surge and sway)

A comparison was done between one single-beam SONAR and two single-beam SONARs (Fig. 2) for 2 DOF localisation. In the case of one single-beam SONAR for localisation, the sensor was placed parallel to the trajectory and during the use of two single-beam SONARs for localisation, both were perpendicular to one of the walls of the diving pool. In both scenarios, the experimental rig was moving in a linear trajectory making an angle of 45^0 (clockwise) with the pool walls.

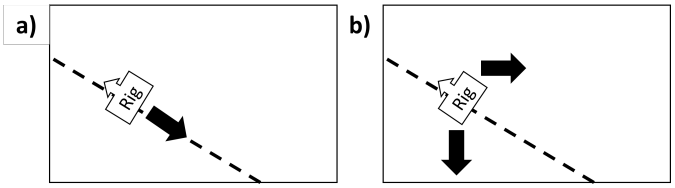

Fig. 2. Arrangement of single-beam SONARs (black) with respect to the experimental rig; a) One SONAR placed parallel to the rig's trajectory ; b) SONARs placed perpendicular to the pool walls

The experimental rig was manufactured from aluminium beams and buoyancy foam (Fig. 3). The foam helped keep the non-waterproofed electronics like the data-logger (Raspberry Pi 4 [18]) and the IMU afloat. The beams also helped attach eye hooks above the foam and other sensors like the TOF sensor above water and the SONARs (1m) as well as the depth sensor (0.6m) underwater.

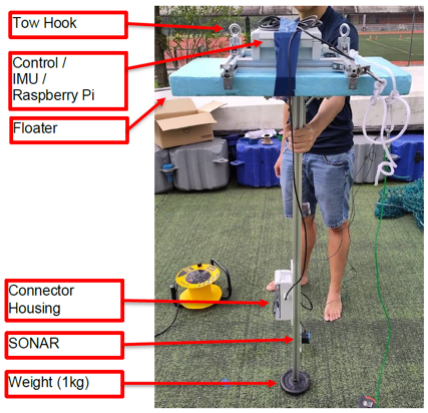

Fig. 3. The experimental rig and its components

To ensure repeatability, the experimental rig was tied by two nylon ropes on either sides and was wound twice on the motorized pulley. Fig. 4 depicts the opposing forces that helped in reducing unwanted sway, thereby guaranteeing repeatability in experiments.

A transmission system was designed for constant velocity movement of a rig containing the localisation sensors (Fig. 5). using a stepper motor. The other elements of the transmission system were designed with the help of a rope spool and an enclosure built using sheet-metal bending. Most experiments were done with with a delay of 1000ms per step. This speed was chosen after analysing the distance readings of the SONAR when the rig was moved with different speeds (Fig. 6).

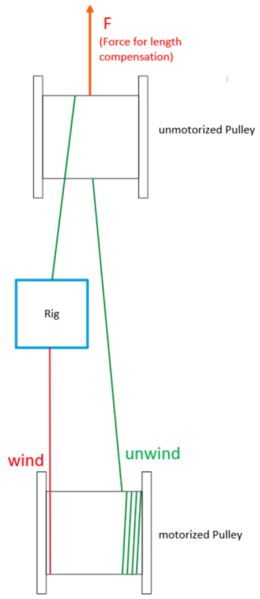

Fig. 4. Detailed configuration of rig with pulleys

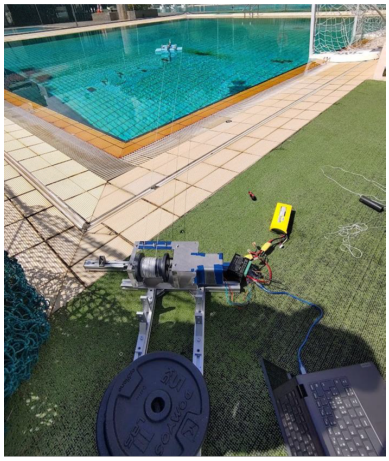

Fig. 5. Final experimental setup. The transmission system moves the rig in precise steps

The experiments were conducted in a diving pool which was 13m (L) x 12m (B) (Fig. 7). The deepest point in the pool is at 4m. Due to varying pool depths, some of its walls were sloped.

Each experimental run was as follows:

1) Move rig for 1m (2 DOF) or 2m (1 DOF)
2) Stop rig for 5s
3) Move rig for 1m (2 DOF) or 2m (1 DOF)
4) Stop rig

B. Linear KF

The linear KF [19] is an algorithm utilized for estimating the state of a linear dynamic system. Currently, the KF is used

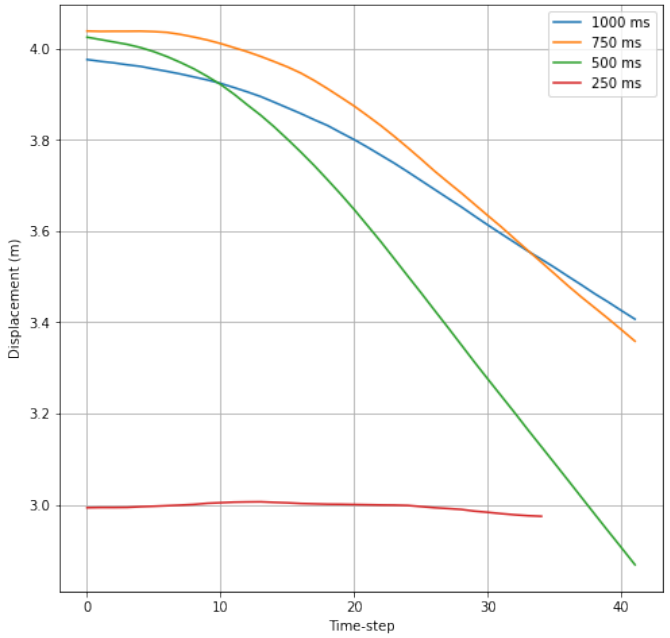

Fig. 6. Effects of speed of rig on SONAR distance readings; 4 speeds tested- 0.06m/s (1000ms delay), 0.09m/s (750ms delay), 0.12m/s (500ms delay) and 0.19m/s (250ms delay)

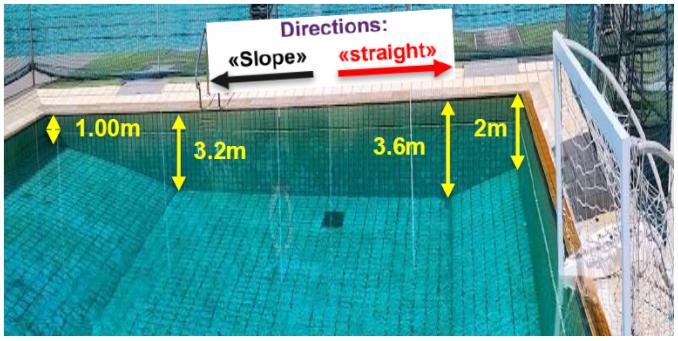

Fig. 7. Diving pool used for experiments

offline and not recursively during the experiments.

Two sets of equations are used in a KF, one to estimate the next state, i.e. the values of displacement and velocity from the IMU and the other to correct these states with the measurements or readings from a reliable source, i.e., from a sensor like the single-beam SONAR.

- Prediction step:

$$\bar{\mathbf{x}_k} = F\mathbf{x_{k-1}} + B\mathbf{u}_k \tag{1}$$

$$\bar{P_k} = FP_{k-1}F^T + Q \tag{2}$$

Where

- $\bar{\mathbf{x}_k}$: Priori state estimate
- $\mathbf{x_{k-1}}$: Posteriori state estimate
- F, F^T: State transition matrix and its transpose
- B: Control Matrix, due to external factors
- $\mathbf{u}_k$: Control vector
- $\bar{P_k}$: Priori covariance error at instance k
- P_k: Posteriori covariance error at instance $k-1$
- Q: Process noise covariance, usually Gaussian in nature

- Update step:

$$\mathbf{y}_k = \mathbf{z}_k - H\bar{\mathbf{x}_k} \tag{3}$$

$$K_k = \frac{\bar{P_k}H^T}{\left(H\bar{P_k}H^T + R\right)} \tag{4}$$

$$\mathbf{x}_k = \bar{\mathbf{x}_k} + K_k\mathbf{y}_k \tag{5}$$

$$P_k = \left(\mathbb{I} - K_kH\right)\bar{P_k} \tag{6}$$

Where-

- $\mathbf{y}_k$: Measurement residual at instance k
- $\mathbf{z}_k$: Measurement vector, at instance k
- H and H^T: Observation matrix and its transpose
- K_k: Kalman gain at instance k
- R: Measurement noise covariance, usually Gaussian in nature

Terms without a subscript do not change with respect to time. The most important term in this process is the Kalman gain (4), as this decides the final value of the estimate. A high gain value implies only the measured value is used for state estimation, i.e., only the SONAR range values and the other derived variables instead of the IMU readings and vice-versa.

The quantities that need to be estimated are the velocity and displacement of a UWR. In the vector form, the equations are:

$$\begin{pmatrix}\mathbf{x}_k\\ \mathbf{v}_k\end{pmatrix} = \begin{pmatrix}1 & \Delta t\\ 0 & 1\end{pmatrix}\begin{pmatrix}\mathbf{x}_{k-1}\\ \mathbf{v}_{k-1}\end{pmatrix} + \begin{pmatrix}0.5(\Delta t)^2\\ \Delta t\end{pmatrix}\left(\mathbf{a}_{k-1}\right) \tag{7}$$

Where $\mathbf{a}$, $\mathbf{v}$ and $\mathbf{x}$ are acceleration, velocity and displacement, respectively. Between time instances k and $k-1$ is the time difference of Δt. The initial conditions used for the filter are:

- $\mathbf{x}_0 = \begin{pmatrix}0 & 0\end{pmatrix}^T$
- $P = Q = 0.01 \times \mathbb{I}_{2\times 2}$

When two single-beam SONARs were used, the components of the linear acceleration outputs from the IMU were transformed as follows:

$$\mathbf{a} = \begin{pmatrix}cos\theta & -sin\theta\\ sin\theta & cos\theta\end{pmatrix}\mathbf{a_{k-1}} \tag{8}$$

The value of θ was constant, which can be observed by the orientation values from the IMU. For all three axes, the angle of rotation was recorded to be 0 with standard deviation in the order of 10^{-5}.

C. Data post-processing

Before fusing the raw data from the IMU and the single-beam SONAR with the KF, some basic filtering was applied to improve the performance of the data fusion. Displacement and calculated velocity (via differentiation) were the quantities obtained from the SONAR, while acceleration and displacement

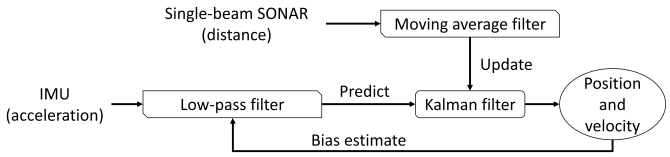

Fig. 8. The filtering process. Raw data from sensors are pre-processed before being used recursively by the KF.

(via double integration) were the quantities obtained from the IMU. Fig 8 shows how the filtering process works.

For the IMU, a 4^{th}-order Butter-Worth low-pass filter was used to reduce the high-frequency noise present in the measurements. A heuristically determined cut-off frequency of 5 Hz was selected to retain important data. Additionally, the bias drift was reduced by evaluating if the acceleration, calculated from velocity is below the actual IMU acceleration. If this case is true, then the current acceleration values will replace the bias measurement.

The single-beam SONAR readings were filtered with two methods, gating and the application of a moving average filter. A moving average filter was applied on the data to ensure its consistency, while gating evaluates if a given distance is acceptable. It decides if a distance measurement was outside the expected range of measurements or if the confidence of the reading, an additional output from the SONAR was below 100% for the current instance. Such outliers are ignored by the KF. This was implemented in the KF by manipulating the measurement noise covariance matrix R (4) as follows:

- For good SONAR readings, covariance will be less, therefore $R = 0.01 \times \mathbb{I}_{2\times 2}$
- For poor SONAR readings, covariance will be high, therefore $R = 10 \times \mathbb{I}_{2\times 2}$

IV. Results

A. 1 DOF localisation

With reference to Fig 1a, using one single-beam SONAR works well to localise the experimental rig with the help of a linear KF for 1 DOF movement (Fig. 9). Table I shows the comparison of some experimental runs with respect to the ground truth.

TABLE I
Errors from experiments; 1 DOF experiment

Position estimation method	Mean RMSE (m)	Mean distance from final position (m)	Standard deviation from final position (m)
IMU	14.248	20.136	6.327
SONAR	0.568	0.08	0.055
KF	0.103	0.079	0.055

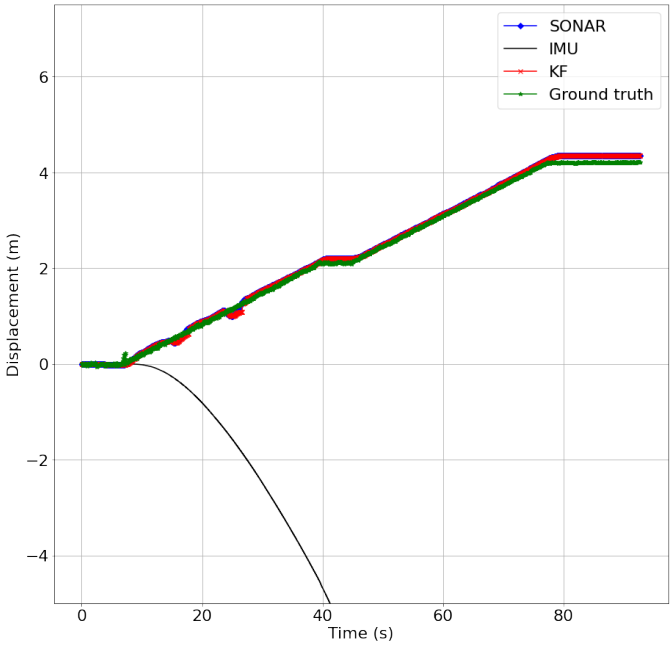

Fig. 9. 1 linear DOF localisation performance using a single-beam SONAR and IMU with a linear KF

TABLE II
Errors from experiments; 2 DOF experiment, one single-beam SONAR

Position estimation method	Mean X position RMSE (m)	Mean Y position RMSE (m)	Mean distance from final position (m)	Standard deviation of final position (m)
IMU	3.387333	3.358	11.79	2.738
SONAR	0.339	0.339	0.502	0.317
KF	0.325	0.319	0.178	0.212

B. 2 DOF localisation

With reference to Fig 1b, the experimental rig was moved diagonally to simulate movement in 2 DOFs. The TOF sensor, due to its limited FOV can no longer be utilized as a source of ground truth, hence it was replaced with stepper motor inputs.

Using two single-beam SONARs significantly improved the localization results when compared with that of one single-beam SONAR (Figs 10 and 11). Tables II and III show the comparison of some experimental runs with respect to the ground truth trajectories.

C. Depth

Depth readings were supposed to be constant as there was no movement in this DOF. The depth sensor provided a reading similar to its placement on the experimental rig, i.e. 0.6m (table IV and Fig 12).

V. Conclusions

Single-beam SONARs are viable alternatives for UWR localisation, at least for the linear DOFs. The distance data

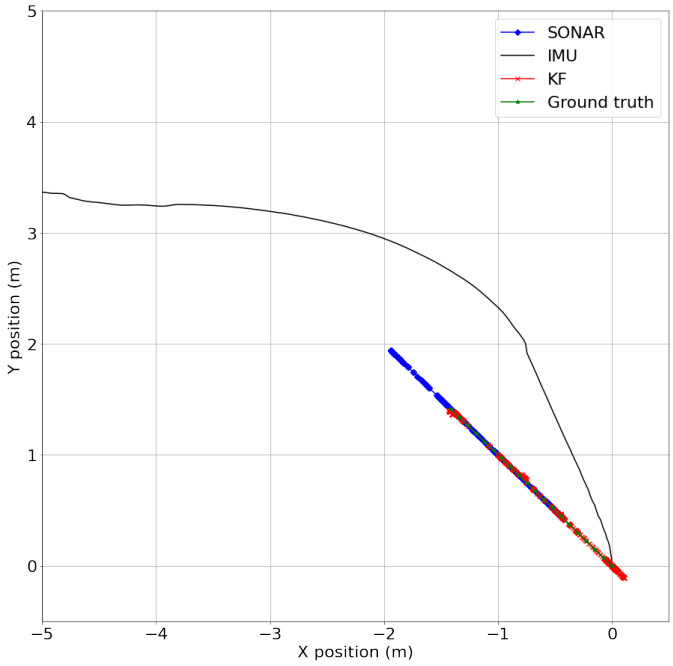

Fig. 10. 2 linear DOF localisation performance using one single-beam SONAR and IMU with a linear KF

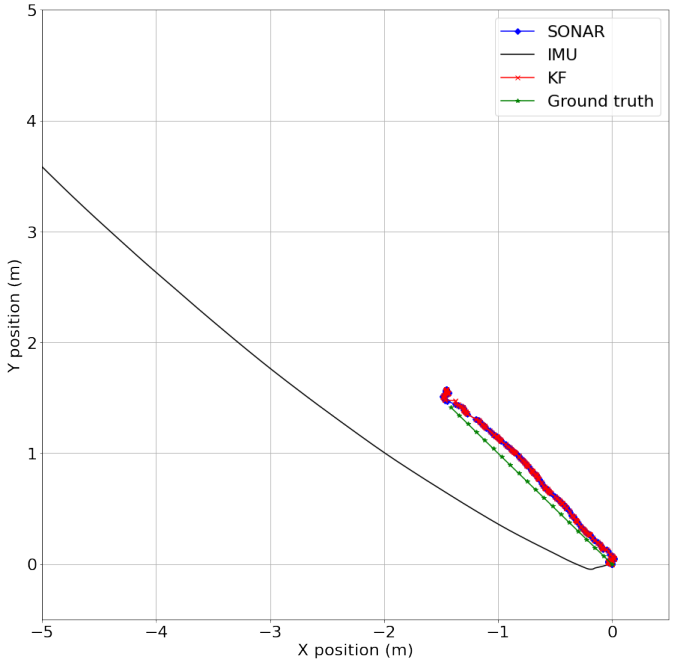

Fig. 11. 2 linear DOF localisation performance using two single-beam SONARs and IMU with a linear KF

TABLE III
ERRORS FROM EXPERIMENTS; 2 DOF EXPERIMENT, TWO SINGLE-BEAM SONARS

Position estimation method	Mean X position RMSE (m)	Mean Y position RMSE (m)	Mean distance from final position (m)	Standard deviation of final position (m)
IMU	3.01	4.364	13.276	6.863
SONAR	0.217	0.186	0.15	0.016
KF	0.16	0.185	0.15	0.016

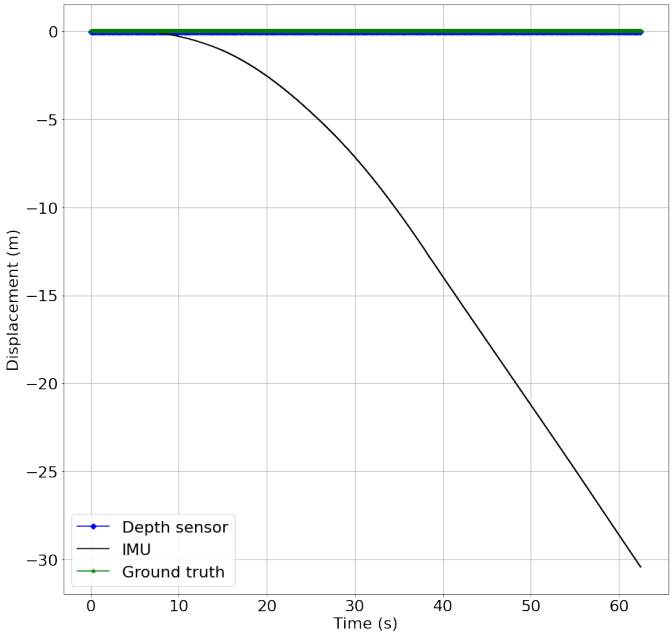

Fig. 12. Depth readings from depth sensor

it provided was used to correct dead-reckoning data from the IMU. As these SONARs are inexpensive compared to its other variants or navigational devices, multiples of such, can be utilized to realize low-cost UWR localisation. Based on the experiments conducted, one single-beam SONAR was required to achieve reliable localisation per DOF.

There are several experiments that need to be conducted to investigate the limitations of these SONARs. For example, the localisation system needs to be evaluated in unstructured environments like lakes. As the experiments in this study were

TABLE IV
ERRORS FROM EXPERIMENTS; DEPTH SENSOR READINGS

Depth estimation method	Mean depth (m)	Standard deviation (m)
Depth sensor	0.0107	0.0002
IMU	5.625	5.664

controlled, the effects of varying UWR speeds, materials and inclination of boundaries on SONAR readings were not fully explored. Moreover, Unlike DVLs, these SONARs assume a speed of sound underwater to derive distance, hence the value of speed must be altered based on the salinity and temperature of the water to get accurate distance readings.

ACKNOWLEDGMENTS

This paper is done as part of the work conducted under the SAAB-NTU Joint Lab with support from SAAB Singapore Pte. Ltd, SAAB AB, NTU Robotics Research Centre (RRC) and NTU Sports and Recreational Centre (NTU-SRC). The authors are grateful to Dr. Jovice Ng of SAAB Singapore for her valuable advice and comments.

REFERENCES

[1] D. Q. Huy, N. Sadjoli, A. B. Azam, B. Elhadidi, Y. Cai, and G. Seet, "Object perception in underwater environments: a survey on sensors and sensing methodologies," *Ocean Engineering*, vol. 267, p. 113202, 1 2023.

[2] "Ping sonar echosounder for underwater distance measurement."

[3] M. Caccia, G. Veruggio, G. Casalino, S. Alloisio, C. Grosso, and R. Cristi, "Sonar-based bottom estimation in uuvs adopting a multi-hypothesis extended kalman filter," *International Conference on Advanced Robotics, Proceedings, ICAR*, pp. 745–750, 1997.

[4] M. Caccia, G. Casalino, R. Cristi, and G. Veruggio, "Acoustic motion estimation and control for an unmanned underwater vehicle in a structured environment," *IFAC Proceedings Volumes*, vol. 30, pp. 41–46, 9 1997.

[5] M. Caccia and G. Veruggio, "Acoustic motion estimation and guidance for unmanned underwater vehicles," *International Journal of Systems Science*, vol. 30, pp. 929–938, 1999.

[6] N. Fairfield, G. Kantor, and D. Wettergreen, "Towards particle filter slam with three dimensional evidence grids in a flooded subterranean environment," *Proceedings - IEEE International Conference on Robotics and Automation*, vol. 2006, pp. 3575–3580, 2006.

[7] N. Fairfield, G. Kantor, and D. Wettergreen, "Real-time slam with octree evidence grids for exploration in underwater tunnels," *Journal of Field Robotics*, vol. 24, pp. 03–21, 2007.

[8] P. Calado, R. Gomes, M. B. Nogueira, J. Cardoso, P. Teixeira, P. B. Sujit, and J. B. Sousa, "Obstacle avoidance using echo sounder sonar," *OCEANS 2011 IEEE - Spain*, 2011.

[9] S. K. Kartal, R. Hacıoğlu, K. S. Görmüş, H. Kutoğlu, and M. K. Leblebicioğlu, "Modeling and analysis of sea-surface vehicle system for underwater mapping using single-beam echosounder," *Journal of Marine Science and Engineering 2022, Vol. 10, Page 1349*, vol. 10, p. 1349, 9 2022.

[10] Y. T. Tan, M. Chitre, and F. S. Hover, "Cooperative bathymetry-based localization using low-cost autonomous underwater vehicles," *Autonomous Robots*, vol. 40, pp. 1187–1205, 10 2016.

[11] N. Osterman and C. Rhen, "Exploring the sensor requirements for particle filter-based terrain-aided navigation in auvs," *2020 IEEE/OES Autonomous Underwater Vehicles Symposium, AUV 2020*, 9 2020.

[12] C. Morency and D. J. Stilwell, "Evaluating the benefit of using multiple low-cost forward-looking sonar beams for collision avoidance in small auvs," *IEEE International Conference on Intelligent Robots and Systems*, vol. 2022-October, pp. 8423–8429, 2022.

[13] M. Roznere and A. Q. Li, "Underwater monocular image depth estimation using single-beam echosounder," *IEEE International Conference on Intelligent Robots and Systems*, pp. 1785–1790, 10 2020.

[14] P. Yang, H. Liu, M. Roznere, and A. Q. Li, "Monocular camera and single-beam sonar-based underwater collision-free navigation with domain randomization," pp. 85–101, 2023.

[15] "Witmotion wt901c rs232 9 axis imu sensor tilt angle roll pitch yaw + acceleration + gyroscope + magnetometer m."

[16] "Tofsense – nooploop."

[17] "Ultra-high resolution pressure/depth sensor for 10m depth."

[18] "Buy a raspberry pi 4 model b – raspberry pi."

[19] S. Thrun, W. Burgard, and D. Fox, *Probabilistic robotics (intelligent robotics and autonomous agents series)*, vol. 45. 2005.